COVER SHEET

Synthesis and characterization of delaminated iron-pillared clay with meso-microporous structure

Peng Yuan,[1,*] Hongping He, [1] Faïza Bergaya,[2,*] Daqing Wu,[1] Qin Zhou,[1] and Jianxi Zhu[3]

1 Guangzhou Institute of Geochemistry, Chinese Academy of Sciences, Wushan, Guangzhou 510640, China

2 Centre de Recherche sur la Matière Divisée, CNRS-Université d'Orléans, 1b, rue de La Férollerie, Orléans Cedex 2, 45071, France

3 Department of Environment Science, Zhejiang University, Hangzhou 310028, China

Abstract

In the present work, iron pillared clays were synthesized by the reaction of montmorillonite with base-hydrolyzed solutions of Fe(III) nitrate. In contrast with the classical microporous pillared structure, a novel meso-microporous delaminated structure containing pillared fragments in iron-pillared clay was obtained. A considerable amount of NO_3^- is found to be retained in the resultant delaminated iron-pillared clays even after thorough washing by successive agitations/centrifugations. This amount is closely related with the content of the iron species in the iron-pillared clays. The highest BET specific surface area and the largest porosity of the delaminated iron pillared clays are 215.7 m^2/g and 0.29 ml/g, respectively. Mesopores in the delaminated structure make the main contribution to the total surface area and porosity, and most of them are preserved after calcination at 773 **K**. These fundamental results are of importance in developing novel heterogeneous catalysts and adsorbents.

Keywords: Iron-pillared clay; Intercalation; Delaminated clay; Meso-microporous structure; Mesoporous materials

1. Introduction

Clays pillared with interlayer inorganic particles (PILC), first reported in the late 1970s [1,2], are prepared by exchanging the interlayer charge compensating cations of clay with larger polymeric or oligomeric hydroxy metal cations formed by hydrolysis of metal salts. By heating temperature greater than 573 K, the intercalated metal hydroxy cations undergo dehydration and dehydroxylation and are converted to metal oxide (e.g. Al_2O_3, TiO_2, and Fe_2O_3) clusters acting as pillars to prop the clay layers apart [3], thus creating a stable microporous system in the interlamellar space of clay particle. These microporous PILCs have been the subject of a large amount of research interest due to their excellent properties as adsorbents and catalysts [3-5].

Most of the metal-oxide pillared clays reported in the literature exhibit basal spacings less than 2 nm, corresponding to interlamellar heights less than 1 nm [6]. However, PILCs with pillars substantially larger than the thickness of silicate layers (*ca.* 1 nm), so called

* Corresponding author. *E-mail address*: yuanpeng@gig.ac.cn (P. Yuan) Tel: +86 20 85290341; Fax: +86 20 85290130.
or *E-mail address*: f.bergaya@cnrs-orleans.fr (F. Bergaya) Tel: 02 38255372; Fax: 02 38633796.

'supergallery' PILCs [7], have attracted much interest in recent years. This is because they can provide larger pore sizes, which in turn extend their applicability as catalysts and shape-selective adsorbents to larger guest species [6-8]. Developments in creating a mesoporous structure in the space between the clay layers by templating with a surfactant have been reported [9-12].

Mandalia et al. reported a high *d*-spacing (ca. 7.6 nm in the XRD pattern of Fe-pillared montmorillonite) without incorporation of any surfactant or other organic polymeric compounds [13]. This *d*-spacing is obviously larger than those of Fe-pillared clays in previous reports (less than 2.95 nm) [5]. Image analysis demonstrated that this *d*-spacing should be assigned to a correlation between pores containing iron aggregates and iron-exchanged clay particles rather than to a d_{001} pillared distance [14]. Accordingly, an interesting question arises, i.e., what are the factors resulting in such a high *d*-spacing of the Fe-PILCs? Especially, what characteristics would be displayed in the porous structure corresponding to such high *d*-spacings?

In this study, a series of Fe-montmorillonites were synthesized with different OH/Fe molar ratios and the resultant products were investigated using powder X-ray diffraction (XRD), nitrogen adsorption-desorption isotherms and Fourier transform infrared spectroscopy (FTIR). Our results show that a novel kind of meso-microporous structure is obtained. Analysis of the relationship between the high *d*-spacing and the mesoporosity of the resultant Fe-montmorillonite provides a new insight into the structure of the PILC. The fundamental information derived from this study is of importance in developing novel catalysts or adsorbents with anions exchangeability.

2. Experimental

2.1 Materials.

The starting calcium-montmorillonite (Ca^{2+}-Mt) was supplied by Nanhai Mining Ltd., China. It was purified and classified by sedimentation, and the < 2 μm fraction was collected. The chemical formula of the obtained Ca^{2+}-Mt can be expressed as:

$$Ca_{0.19}Mg_{0.06}Na_{0.01}(Si_{3.96}Al_{0.04})\ (Al_{1.44}Fe_{0.09}Mg_{0.47})\ O_{10}(OH)_2{\cdot}nH_2O.$$

Its cationic exchange capacity (CEC) is 66.5 mmol/100g. Na^+-activated montmorillonite (Na^+-Mt) was prepared by ion exchange reaction between Ca^{2+}-Mt and Na_2CO_3, as previously described [15]. Both Ca^{2+}-Mt and Na^+-Mt were used as the starting materials for the pillaring reactions.

The Keggin-type heteropolyanion $[PW_{12}O_{40}]^{3-}$ was prepared by titration of the $H_3PW_{12}O_{40}$ solution (pH ca. 2.0) with a solution of NH_4OH.

2.2 Preparation of Iron Pillaring Solutions.

Following a procedure similar to the one reported by Rightor *et al*. [16], Na_2CO_3 powder was added slowly to an aqueous solution of 0.2 M iron (III) nitrate with vigorously stirring (ca. 1100 revs/min). The amount of added base was up to six OH/Fe molar ratios which are in the range of 0.5 - 2.5. The resulting translucent solution was aged for 24 h at room temperature before being added to the montmorillonite dispersion.

2.3 Pillaring Process.

A dispersion of 2 g of purified montmorillonite in 100 ml of deionized water was used. The iron pillaring solution was added dropwise into the vigorously stirred clay suspension kept in a water bath at 333 K, with a ratio of Fe: clay = 10 mmol g^{-1} of clay. After addition of the pillaring solution, the reaction mixture was stirred for an additional 2 h, and aged for 20 h at room temperature. The mixture was centrifuged and washed 12 times by successive agitations/centrifugations with deionized water. The product was air-dried at 378 K for 16 h and ground into powder for further characterizations. The final PILC products were differentiated on the basis of the kind of starting montmorillonite and of the OH/Fe molar ratio. For instance, Na^+-Mt-1.0 corresponds to a sample of Na^+-Mt treated with a pillaring solution with the molar ratio OH/Fe = 1.

2.4 Exchange Reaction.

The exchange reaction between the Keggin-type heteropolyanions $[PW_{12}O_{40}]^{3-}$ and the iron-pillared sample was carried out by titrating the $[PW_{12}O_{40}]^{3-}$ solution into the Na^+-Mt-1.0 (wet cake) in a ratio of heteropolyanions/ Na^+-Mt-1.0 = 2mmol/5g. The mixture was then stirred for 3 h at 353 K. The product was separated by centrifugation, washed with deionized water, and dried at 378 K for 16 h.

2.5 Characterization.

The chemical composition of the samples was determined using an PE-3100 atomic absorption spectrometer (AAS). A Rigaku D/max 2550 PC X-ray diffractometer (CuKα radiation, λ = 0.154 nm) equipped with a graphite monochromator was used to acquire the XRD patterns of the powdered samples (0.5 - 12^o (2θ). A fixed power source (40 kV, 300 mA), and a scan rate of 3 deg (2θ)/min were applied for the determination of XRD.

The FTIR spectra of the samples were recorded on a Perkin-Elmer 1725X FTIR spectrometer. Specimens for measurement were prepared by mixing 0.9 mg of the sample powder with 70 mg of KBr and by pressing the mixture into a pellet. The average over 9 scans was collected for each measurement in a wavenumber range of 300 - 4000 cm^{-1} with a resolution of 2 cm^{-1}.

N_2 adsorption-desorption isotherms were measured at liquid nitrogen temperature with a gas sorption analyzer (Quantachrome, NOVA 1000). Prior to measurement, samples were outgassed at 523 K, at a pressure less than 10^{-3} Torr for at least 3 h. The specific surface area was calculated by the BET equation and the total pore volume was evaluated from nitrogen uptake at a relative pressure of 0.985 [17]. The *t*-plot according to De Boer's method was used to calculate the micropore volume and external surface area [18]. The Barrett-Joyner-Halenda (BJH) method was used to evaluate the average pore diameter (APD) [19].

3. Results

3.1 Chemical Analysis.

The main compositions of Fe-pillared clays, presented as mass percentage of oxides, are summarized in Table 1. The molar content of iron per $O_{10}(OH)_2$ unit is also given, based on the

assumption that the Al_2O_3 content in montmorillonite is unchanged during the pillaring reaction.

The pH values of 24h-aged pillaring solutions are 1.64, 1.66, 1.67, 1.70, 1.72 and 1.90, and those of the final 20h-aged pillaring mixtures are 1.53, 1.56, 1.58, 1.64, 1.70 and 1.95, corresponding respectively to the OH/Fe molar ratios of 0.5, 0.8, 1.0, 1.5, 2.0, and 2.5. This result is analogous to that reported by Rightor *et al*. [16]. It can be seen that increase of OH/Fe molar ratio in the initial pillaring solution results in a remarkable increase of the iron content of the iron-pillared products. In addition, the iron content of Fe-pillared Na^+-Mt is considerably higher than that of Fe-pillared Ca^{2+}-Mt.

3.2 FTIR Spectra.

Figure 1 shows the FTIR spectra of the initial montmorillonite and treated clay samples. The wavenumber and assignment of the vibration modes observed are listed in Table 2. The assignments are based on previous reports on montmorillonite and polyoxometalates samples [20,21].

As shown in Figure 1, a vibration mode at ca. 1384 cm^{-1}, attributed to the NO_3^- stretching mode, is observed in the FTIR spectra of PILC synthesized from Na^+-Mt. It is of particular interest that the intensity of that peak strongly depends on the OH/Fe molar ratio: an increase of the OH/Fe ratio from 0.5 to 2.5 (Figure 1, B - G) leads to a stepwise increase of peak intensity. A dramatic increase is observed as the OH/Fe ratio increases from 0.8 to 1 (Figure 1, C and D). A similar correlation could also be found between the intensity of NO_3^- band and the content of iron (Table 1). The NO_3^- band is however not observed in the spectra of Fe-pillared Ca^{2+}-Mt samples (Figure 1, I and J).

If the pillaring of the iron species in the interlayer spaces of montmorillonite is followed by a typical ion exchanged process as reported in the literature [16], the NO_3^- should be removed from the final product after the successive agitations/centrifugations. Accordingly, the occurrence of the NO_3^- band suggests that there might exist some redundant positively charged iron species outside the interlayer of Na^+-Mt, and that the NO_3^- anions act as counterions to balance the positive charge of the iron species. For Fe-pillared Ca^{2+}-Mt, however, the amount of redundant iron species seems to be very small, resulting in a negligible content of NO_3^- counterions.

In the FTIR spectrum of Na^+-Mt-heteropolyanions (Figure 1K), the NO_3^- band at 1384 cm^{-1} disappears whereas the main vibration modes of $[PW_{12}O_{40}]^{3-}$ appear. This suggests that, in this sample, NO_3^- initially present in Na^+-Mt-1.0 has been replaced by $[PW_{12}O_{40}]^{3-}$.

3.3 XRD Analysis.

Two peaks were observed in the XRD patterns of the initial Na^+-Mt and its corresponding pillared samples (Figure 2, A-H). The first peak corresponds to a large *d*-spacing greater than 6.4 nm, and the second one to a small *d*-spacing less than 1.59 nm. An increase of the molar ratio of OH/Fe in the pillaring solutions leads to (i) a large *d*-spacing fluctuation between 6.5 and 7.2 nm, and (ii) a shift of the small *d*-spacing from 1.25 (Na^+-Mt) to ca. 1.58 nm, as presented in Table 3.

It is interesting that both the initial Na^+-Mt and Ca^{2+}-Mt show unexpected large *d*-spacing (Figure 2, A and B). The large *d*-spacing of Ca^{2+}-Mt, as well as those of pillared samples (Figure 2, C - J), show good duplicability in repeated analyses. However, the peak of the large

d-spacing in the XRD pattern of Na^+-Mt exhibits obvious variations in intensity, depending on the exposure time of Na^+-Mt sample to air. The XRD pattern in Figure 2A corresponds to a Na^+-Mt sample with the largest peak intensity of the large *d*-spacing. This suggests that Na^+-Mt is very sensitive to ambient relative humidity. The first peak with a large *d* value in pillared samples was analogous to that reported by Mandalia et al [13]. These authors observed a *d*-spacing of *ca.* 7.6 nm in the XRD pattern of Fe-pillared montmorillonite with an OH/Fe ratio of 1.0, and a *d*-spacing of ca. 7.2 nm for mixed Al-Fe pillared sample with a Fe/(Al + Fe) molar ratio of 0.5 and an OH/(Al+Fe) ratio of 1.0. It was proposed that the peak at ca. 7.6 nm could be interpreted as a large interlayer repeat distance [13]. However, in their further studies on the structure of the above-mentioned Al-Fe pillared samples by high-resolution transmission electron microscopy (HRTEM), Clinard et al. proposed that the 7.2 nm peak cannot be attributed to simple intercalation [14], but rather that this peak might be the result of the distribution of pores, as previously shown in some porous solids [22].

However, in the present work, the large *d*-spacing was observed in the XRD pattern of the initial montmorillonite. This strongly supports that the large *d*-spacing does not result from the periodic structure of iron species intercalated into the host montmorillonite, but reflects the existence of a highly correlated porous structure in the starting montmorillonite, as observed in some disordered porous solids such as Vycor glass [22], mesoporous silica molecular sieves [23,24] and mesoporous TiO_2 [25].

The porous structure ("house of cards" structure) in Na^+-Mt is formed by the aggregation of clay particles [26,27]. The fact that the *d*-spacing of ca. 7.36 nm for Ca^{2+}-Mt is considerably smaller than the one in Na^+-Mt suggests that the porous structure might more easily be formed in Na^+-Mt. Unlike this purified Ca^{2+}-Mt, a natural Ca^{2+}-Mt sample from the Hebei province (China) shows an XRD pattern without the large *d*-spacing (Figure 2K), whereas its derived Na^+-Mt exhibits a large *d*-spacing at 7.6 nm (not shown here), similar to the one at 8.2 nm of the Na^+-Mt used for pillaring in this study. This observation indicates that the water treatment process, especially for the Na^+-activated process, might have a prominent influence on the structure of powdered montmorillonite.

The resulting iron-pillared samples also exhibit reflections with large *d*-spacings, indicating the existence of correlated porous structures. This porous structure could result from the three-dimensional aggregation of clay particles and iron hydroxycations, rather than from a system formed by the intercalation of iron species in the interlamellar space. This is supported by the presence of NO_3^- counterions in the pillared clay minerals.

The broad peak at ca. 1.5 nm in the XRD pattern should be attributed to the *d*(001) value of iron-pillared clays resulting from the periodic stacking of clay layers. The increase of the *d*(001) value from 1.25 nm for the starting Na^+-Mt (Figure 2A) to ca. 1.5 - 1.6 nm for pillared clays indicates the occurrence of intercalation of small size Fe^{3+} hydrolysis products in the clay interlamellar space. This is consistent with the HRTEM observation of a wide distribution of *d*(001) values with a mean value of 1.58 ± 0.10 nm, reported by Clinard et al [14].

As shown in Figure 2, the intensity of the (001) reflection decreases with an increase of the content of iron species introduced, reflecting the decrease of stacking regularity of the pillared clays. This suggests that hydrated iron species could aggregate together and become larger in size at higher OH/Fe ratio [28-31], resulting in the delamination of some host clay particles and in the absence of long range face-to-face stacking of the clay layers.

3.4 Nitrogen Adsorption-Desorption Isotherms.

Figure 3 represents the nitrogen adsorption-desorption isotherms of the initial Na^+-Mt and of iron-pillared clays. The adsorption isotherm of Na^+-Mt (Figure 3A) is Type III (BDDT classification [32]), characteristic of nitrogen adsorption on macroporous adsorbents. The adsorption isotherms of iron-pillared clays is rather type IV, corresponding to mesoporous adsorbents. This suggests that the mesoporosity constitutes most of the total porosity. In addition, iron-pillared clays (Figure 3, B - H) present Langmuir adsorption isotherms (type I) in the region of low relative pressure, indicating the presence of micropores. The hysteresis loops of these isotherms seem to be of type H3 (IUPAC classification [17]), corresponding to slit-shaped pores in layered materials.

The structural parameters of the pore structure, including specific surface areas (S_{BET}), external surface areas (S_{ext}), total porous volume (V_P), microporous volume ($V_{\mu P}$) and average pore diameter (APD), are summarized in Table 3. The iron pillared clays exhibit developped porosity and surface area as compared with the starting montmorillonite. The largest surface area (215.7 m^2/g) and V_P (0.29 ml/g) are found in Na^+-Mt-1.0. Pillared clays synthesized from Na^+-Mt show a more highly developed porosity and surface area than those obtained from Ca^{2+}-Mt. For the pillared clays synthesized from Na^+-Mt, S_{BET} as well as V_P show a remarkable increase whereas the APD decreases when the OH/Fe ratio increases from 0.5 to 1.0. However, an increase from 1.5 to 2.5 of the OH/Fe ratio has little effect on the pore structure parameters of the resulting clays (Table 3).

The porosity of initial montmorillonite results from a “house of cards” structure [26]. In the iron-pillared clays, clay particles and some hydrated iron cations outside the clay interlamellar space could overlap, forming a secondary “house-of-card” porous structure. As a result, the mesoporosity would result from the interspaces of the overlap. The microporosity could have two possible sources: one is resulting from the intercalation of primary hydrolysis products of small size iron cations, and the other the interstices among iron aggregates and/or clay particles, as previously reported [31].

4. Discussion

4.1 Formation of a Delaminated Structure in Iron-Pillared Clays.

Due to the intrinsic catalytic activity (e.g. as a Fischer-Tropsch catalyst) and the potential magnetic properties of iron oxide phases, much interest and research have been directed towards iron oxide PILCs [33-37]. The common route for the synthesis of Fe-PILCs is based on the intercalation of iron polyoxocations [5], resulting from the hydrolysis of Fe(III) salts with a base. In addition, several other studies reported the synthesis of Fe-PILCs by the intercalation of trinuclear Fe(III)-acetato complexes [38-40].

The free interlamellar space heights of Fe-pillared clays synthesized by the hydrolysis of iron salts are variable, as reported in the literature. However, basal spacings of ca. 2.5 ± 0.4 nm were reported by several authors [5,16,41]. Earlier work indicated that the pillared structure was unlikely to be formed via reaction between smectites and hydroxy Fe(III) cations [42]. This is supported by the fact that basal spacings thus obtained are smaller than 1.47nm [34,43-45]. Burch *et al*. [45] and Chen *et al*. [46] proposed that iron-delaminated clay rather than iron-pillared clay were formed in some cases.

The delaminated structure was firstly reported for Al-PILC by Pinnavaia *et al.* [26] and directly observed with HRTEM by Occelli *et al*.[47] This structure was described as a "house of cards" structure, exhibiting an absence or broadening of the 001 X-ray reflection.[26] Freeze-drying, rather than air-drying, was shown to be necessary to obtain a delaminated structure, since air-drying would result in a reorganization of the delaminated aggregates to face-to-face aggregation [26].

It can therefore be concluded that a delaminated structure is formed in the iron-pillared clays. Since these delaminated clays contain pillared fragments, they should be referred to as delaminated iron pillared clays (hereafter noted DIPCs). A noteworthy difference is that this delaminated structure was retained after air-drying, while the delaminated structure of Al-pillared clays previously reported could only be preserved by freeze-drying [26]. A schematic representation of this delaminated-pillared structure is shown in Figure 4.

Few studies were conducted to explain the difference of results on iron PILC reported by different authors under analogous synthetic conditions, i.e., why some authors obtained pillared structure while others obtained delaminated structure. Chen *et al*.[43] proposed that pillared clay resulted from short reaction times (e.g., less than 3 h) at ambient temperature whereas delaminated clay were formed during long reaction time (e.g., over 12 h) and higher temperatures (313 – 323 K). However, Canizares *et al*.[41] did not obtain delaminated clay by a pillaring reaction lasting 12 h. In present work, under a variety of reaction conditions (i.e., changing the reaction time and temperature), we never obtained the pillared structure with a characteristic *d*(001) value larger than 2 nm, as reported in the literature [5,16,41]. This result suggests that a stable iron-pillared structure synthesized by hydrolysis of iron salts might be difficult to obtain, as Herrera *et al*. previously reported [42]. This is not so surprising, since hydrated Fe cations tend to form discrete polyoxocation spheres [48,49], which as a result, do not form ordered pillared structures.

4.2 Formation of Meso-microporous Structures and Effect of OH/Fe Molar Ratios.

The maximum surface area (215.7 m^2/g) found in Na^+-Mt-1.0 is consistent with the values reported for iron PILC [5, 16, 41-46, 50,51]. However, the maximum total porosity (0.29 ml/g) appears higher than the ones reported in the literature [41-46], perhaps because mesoporosity contributes to most of the total porosity in the resultant delaminated pillared structure. This remarkable mesoporosity is of particular significance, since it indicates that the hydrolysis of iron salts could provide an alternative way to obtain a mesoporous structure in pillared clays, besides the approach of surfactant templating [9-12].

The OH/Fe molar ratio of the initial pillaring solution has a prominent influence on the formation of a meso-microporous structure in the DIPCs. At low OH/Fe molar ratios (< 1.0), iron cations are hydrolyzed to primary products with low molecular weight and small size, some of which could be intercalated into the clay interlayer. However, at high OH/Fe molar ratios, hydrated iron cations tend to aggregate [28-31]. The resultant much larger iron aggregates tend to remain outside the interlayer and overlap with the clay particles to form the delaminated structure. Accordingly, some characteristics of the DIPCs, such as mesoporosity/microporosity and the XRD pattern, vary with the OH/Fe molar ratios.

Analysis of the relationship between the high *d*-spacing and the porosity indicates that the starting Na^+-Mt with macropores yields a very intense and symmetric peak with high *d*-spacing. However, meso-microporous pillared/delaminated Na^+-Mt yields a much weaker and broader

peak, with a smaller *d*-spacing. In addition, pillared/delaminated Ca^{2+}-Mt exhibits a much lower surface area and porosity, as well as a much weaker peak with high *d*-spacing, than that is obtained with Na^{+}-Mt. These observations suggest that the XRD pattern at low 2θ angles can provide useful information about the porous structure of clay materials, although the accurate assignment of the high *d*-spacing is difficult.

It is noteworthy that, in previous studies, the scans of the XRD patterns of PILC usually began at ca. 2^{o} (2θ) rather than 0.5^{o} (2θ). However, our observations indicate that a scan beginning at lower 2θ angle is necessary to investigate the structure of PILCs.

4.3 Roles of NO_3^- and Thermal Stability of the Resultant Materials.

In a classical pillared structure of PILC, anions such as Cl^- and NO_3^- would be washed away by repeated agitation and centrifugation. However, a large amount of NO_3^- is retained in the DIPCs of the present work, despite a thorough washing process with twelve or more agitation/centrifugation procedures. The occurrence of NO_3^- therefore supports the proposal of the formation of a delaminated structure. The existence of NO_3^- in the DIPC is of high interest and academic importance, since NO_3^- could be used as an exchanging site for other anions, and the content of NO_3^- could be controlled to some extent by adjusting the OH/Fe ratio. The exchangeability of the NO_3^- by heteropolyanions, e.g. $[PW_{12}O_{40}]^{3-}$ as mentioned above, might be of significance in catalytic application.

Further ongoing work is aimed at investigating the acidity of this novel heteropolyanions-exchanged montmorillonite and exploring its possibility as a heterogeneous catalyst. In contrast with the DIPC derived from cationic montmorillonite, anionic clays such as layered double hydroxides (LDH) are previously known to have the property of anion exchangeability and have been used in the catalytic field [52,53].

After calcination at 773 K for 3h, Na^{+}-Mt-1.0 sample shows an obvious decrease of surface area and microporous volume (Table 3) but most of the mesoporosity is preserved. This is not similar to the behavior reported by Yamanaka et al. [33], in which the iron pillared clays synthesized by hydrolysis of iron salts lack thermal stability above 573 K. Calcination of Na^{+}-Mt-1.0 at 773 K also led to the evaporation and/or decomposition of most NO_3^- and OH^-, as deduced from the FTIR spectra (not shown here), which might result in the formation of Lewis acid sites, based on a previously reported mechanism of Al-PILC [50]. This proposal can well explain the previous report on an unexpected acidity of iron-pillared clay [44], exhibiting a basal spacing of ca. 1.47 nm but containing much more acid sites than in conventional Al-PILC after calcination at 673 K. Hence, this DIPC could prove to have interesting possibilities as a catalyst owing to its thermal stability and anions exchangeability.

5. Conclusions

The hydrolysis of Fe(III) salts with a base was used to synthesize Fe-PILCs. The resulting products are delaminated iron-pillared clays (DIPCs), with a characteristic delaminated mesoporous structure containing Fe-pillared microporous clay fragments. Some novel findings about the DIPC can be summarized as follows:

1) A large *d*-spacing as evidenced in the XRD patterns corresponds to a secondary mesoporous “house of cards” delaminated structure rather than to the periodic intercalated

structure. The mesoporous delaminated structure results from the overlapping between clay particles and the iron aggregates outside the clay interlayer. A large *d*-spacing is observed in the XRD pattern of the initial montmorillonite for the first time, supporting our assignment of the large *d*-spacing to the mesoporous delaminated structure. This study demonstrates that the synthesis method by hydrolysis of iron salts is an alternative way to obtain a mesoporous structure in pillaring solution-treated clays.

2) A large amount of NO_3^- is found to be contained in the mesoporous delaminated structure, with the NO_3^- counterion neutralizing the positive charge of iron aggregates outside the clay interlayer. This anion can be exchanged with heteropolyanions such as $[PW_{12}O_{40}]^{3-}$, and its amount can be controlled by adjusting the OH/Fe molar ratio in the initial pillaring solution.

All these findings suggest that DIPC shows potential applications in many fields (e.g. adsorbent, catalyst, etc.), due to its mixed meso-microporosity, thermal stability and anion exchangeability.

Acknowledgments

Financial supports from Natural Science Foundation (Grant No. 04002140 and 5006267) of Guangdong Province, China, Foundation of Guangzhou Institute of Geochemistry (Grant No. GIGCX-04-02), and National Natural Science Foundation (Grant No. 40372029) of China are gratefully acknowledged. The authors thank Dr R. Setton for improving this manuscript. Grateful thanks are also due to Prof. F. Y. Wang and Dr D. Yang for their assistance to this work.

References

[1] G. W Brindley, R. E. Sempels, Clay Miner. 12 (1977) 229.

[2] N. Lahav, U. Shani, J. Shabtai, Clays Clay Miner. 26 (1978) 107.

[3] R. T. Yang, L. S. Cheng, Access in Nanoporous Materials; Pinnavaia, T. J., Thorpe, M. F., Eds.; Plenum Press: Van Norstrand Reinhold: New York, 1995.

[4] T.J..Pinnavaia, Science. 220 (1983) 365.

[5] J. T. Kloprogge. J. Porous Mater. 5 (1998) 5.

[6] Y.S. Han, J. H. Choy, J. Mater. Chem. 8 (1998) 1459.

[7] A. Moini, T. J. Pinnavaia, J. Solid State Ionics 26 (1988) 119

[8] S.Yamanaka, Y. Inoue, M.Hattori, F. Okumura, M. Yoshikawa, Bull. Chem. Soc. Jpn. 65 (1992) 2494.

[9] C. T. Kresge, M. E.;Leonowicz, W. J. Roth, J. C. Vartuli, J. S. Beck, Nature 359 (1992) 710.

[10] S. Inagaki, Y. Fukushima, K. J. Kuroda, J. Chem. Soc. Chem.Commun. (1993) 680.

[11] A. Galarneau, A. Barodawalla, T. J. Pinnavaia, Nature 374 (1995) 529.

[12] H. Y. Zhu, Z. Ding, J. C. Barry, J. Phys. Chem. B 106 (2002) 11420.

[13] T. Mandalia, M. Crespin, D. Messad, F. Bergaya, J. Chem. Soc. Chem. Commun. (1998) 2111.

[14] C. Clinard, Mandalia, T.; Tchoubar, D.; Bergaya, F. Clays Clay Miner. 51 (2003) 421.

[15] H. P. He, R. L. Frost, F. Deng, J. X. Zhu, X. Y. Wen, P.Yuan, Clays Clay Miner. 52 (2004) 350.

[16] E.G. Rightor, M.S. Tzou, T.J. Pinnavaia, J. Catal. 130 (1991) 29.

[17] S. J. Gregg, K. S. W. Sing, Adsorption, Surface Area and Porosity, 2nd ed.; Academic Press: New York, 1982.

[18] J. H. De Boer, B. G. Linsen, T. Van der Plas, G. J. Zondervan, J. Catal. 4 (1965) 69.

[19] E. P. Barrett, L. G. Joyner, P. P. Halenda, J. Am. Chem. Soc. 73 (1951) 373.

[20] J. Madejova, P. Komadel, Clays Clay Miner. 49 (2001) 410.

[21] C. R. Deltcheff, M. Fournier, R. Franck, R. Thouvenot, Inorg. Chem. 22 (1983) 207.

[22] P. Levitz, D. Tchoubar, J. Phys. 2 (1992) 771.

[23] S. A. Bagshaw, E. Prouzet, T. J. Pinnavaia, Science 269 (1995) 1242.

[24] S. A. Bagshaw, E. Prouzet, T. J. Pinnavaia, Angew Chem. Int. Ed. Engl. 35 (1996) 1102

[25] L. Hu, Q. Yu, B. Deng, R. J.Yu, R. Song, A. W. Xu, Acta Scieniarum Naturalium Universitatis Sunyatseni 43 (2004) 128.(in Chinese)

[26] T. J. Pinnavaia, M. S. Tzou, S. D. Landau, R. H. Raythatha, J. Mol. Catal. 27 (1984) 195.

[27] G. Lagaly, S. Ziesmer, Adv. Colloid Interfac. 100 (2003) 105.

[28] P. J. Murphy, A. M. Posner, J. P. Quirk, J Colloid Interface Sci. 56 (1976) 270.

[29] C. M. Jr Flynn, Chem. Rev. 84 (1984) 31

[30] D. Tchoubar, J. Y. Bottero, P. Quienne, M. Arnaud, Langmuir 7 (1991) 398.

[31] J. Y. Bottero, A. Manceau, F. Villieras, D. Tchoubar, Langmuir 10 (1994) 316.

[32] S. Brunauer, L. S. Demming, W. S. Demming, E. J. Teller, Am.Chem. Soc. 62 (1940) 1723.

[33] S. Yamanaka, T. Doi, S. Sako, M. Hattori, Mater. Res. Bull. 19 (1984) 161.

[34] D. H. Doff, N. H. J. Gangas, J. E. M. Allan, J. M. D. Coey, Clay Miner. 23 (1988) 367.

[35] F. Bergaya, J. Barrault, Pillared Layered structures. Current trends and applications. Mitchell, I. V. Ed.; Elsevier Sc. Publishers: Amsterdam, 1990

[36] F. Bergaya, N. Hassoun, L. Gatineau, J. Barrault, Preparation of Catalysts. V. Poncelet, G. Jacobs, P.A., Grange, P., and Delmon, B., Eds.; Elsevier Sc. Publishers: Amsterdam, 1991.

[37] J. Barrault, L. Gatineau, N. Hassoun, F. Bergaya, Energ Fuel. 6 (1992) 760.

[38] M. A. Martin-Luengo, H. Martins-Carvalho, J. Ladriere, P. Grange, Clay Miner. 24 (1989) 495.

[39] N. Maes, E.F. Vansant, Micropor. Mater. 4 (1995) 43.

[40] L. Huerta, A. Meyer, E. Choren, Micropor. Mesopor. Mater. 57 (2003) 219.

[41] P. Canizares, J. L. Valverde, M. R. S. Kou, C. B. Molina. Micropor. Mesopor. Mater. 29 (1999) 267.

[42] R. Herrera, M. Peech, Soil Sci. Soc. Amer. Proc. 34 (1970) 740.

[43] W. Y. Lee, R. H. Raythatha, B. J. Tatarchuk, J. Catal. 115 (1989) 159.

[44] H. M. Mody, P. M. Oza, V. P. Pandya, J. Indian Chem. Soc. 70 (1993) 11.

[45] R. Burch, C. I. Warburton, Appl. Catal. 33 (1987) 395.

[46] J. P. Chen, M. C. Hausladen, R. T. Yang, J. Catal. 151 (1995) 135.

[47] M. L. Occelli, J. V. Senders, J. Lynch, J. Catal. 107 (1987) 557.

[48] T. G. Spiro, S. E. Allerton, J. Renner, A. Terzis, R. Bils, P. Saltman, J. Am. Chem. Soc. 88 (1966) 2721.

[49] J. M. Oades, Clays Clay Miner. 32 (1984) 49.

[50] T. J. Bandosz, K. Cheng, J Colloid Interface Sci. 191 (1997) 456.

[51] S. Balci, E. Gokcay, Mater. Chem. Phys. 7 (2002) 46.

[52] T. Kwon, T. J. Pinnavaia, Chem. Mater. 1 (1989) 381.

[53] T. Polubesova, T. Undabeyta, S. Nir, L. Chertkova, H. Vandamme, F. Bergaya, J Environ Qual. 29 (2000) 948.

Tables

Table 1: Main chemical composition of iron-pillared clay samples

Table 2: Positions and assignments of observed IR vibration bands

Table 3: XRD spacings (0 – 12^{o} 2θ angle) and textural properties of the initial and treated montmorillonite samples

Table 1
Main chemical composition of iron pillared clay samples

sample	analytical results (%)			mol composition[a]	
	SiO_2	Al_2O_3	Fe_2O_3	Al	Fe
Na^+-Mt –0.5	53.96	10.12	17.83	1.48	1.66
Na^+-Mt –0.8	52.01	9.26	21.17	1.48	2.16
Na^+-Mt –1.0	50.04	8.99	24.84	1.48	2.61
Na^+-Mt –1.5	48.03	8.89	25.36	1.48	2.69
Na^+-Mt –2.0	47.35	8.62	25.53	1.48	2.80
Na^+-Mt –2.5	48.27	8.47	30.06	1.48	3.35
Ca^{2+}-Mt-1.0	56.39	10.71	15.63	1.48	1.38
Ca^{2+}-Mt-2.0	51.81	10.71	18.74	1.48	1.65

[a] The compositions given in moles per $O_{10}(OH)_2$ anion basis of silicate layer.

Table 2
Positions and assignments of the IR vibration bands observed

Position (cm^{-1})	Assignments	Position (cm^{-1})	Assignments
3618	OH stretching of structural hydroxyl groups	982	W=O stretching of $[PW_{12}O_{40}]^{3-}$
3420	OH stretching of water	916	Al-Al-OH deformation
1630	OH deformation of water	883	W-O-W stretching of $[PW_{12}O_{40}]^{3-}$
1435	CO_3 stretching of calcite	799	W-O-W stretching of $[PW_{12}O_{40}]^{3-}$
1384	NO_3 stretching	842	Al-Mg-OH deformation
1092	Si-O stretching of cristobalite	796	Si-O stretching of cristobalite
1081	P-O stretching of $[PW_{12}O_{40}]^{3-}$	624	Coupled Al-O and Si-O, out of plane
1034	Si-O stretching	519	Al-O-Si deformation

Table 3

XRD Spacings (0 – 12^{o} 2θ angle) and textural properties of the initial and treated montmorillonite samples

sample	OH/Fe (**molar ratio**)	First peak (*d*/nm)	Second peak (*d*/nm)	S_{BET} (m^2/g)	[a]S_{ext} (S_{micro}) (m^2/g)	[b]V_P (mL/g)	[c]$V_{\mu P}(V_{\mu P}/V_P)$ (mL/g)	[d]APD (nm)
Na^+-Mt	—	8.20	1.25	35.1	—	0.138	—	15.76
Na^+-Mt –0.5	0.5	6.54	1.47	143.6	113.6 (30.0)	0.224	0.012(5.4%)	6.25
Na^+-Mt –0.8	0.8	7.12	1.59	158.2	116.7 (41.5)	0.230	0.018(7.8%)	5.82
Na^+-Mt –1.0	1.0	6.74	1.54	215.7	139.8 (75.9)	0.291	0.033(11.3%)	5.39
Na^+-Mt –1.5	1.5	7.12	1.58	182.5	120.9 (61.6)	0.245	0.026(10.6%)	5.38
Na^+-Mt –2.0	2.0	6.49	1.57	173.4	116.0 (57.4)	0.235	0.024(10.2%)	5.42
Na^+-Mt –2.5	2.5	7.24	1.58	177.5	111.1 (66.4)	0.228	0.029(12.7%)	5.13
[e]Na^+-Mt –1.0	—	—	—	128.2	102.0 (26.2)	0.196	0.012(6.1%)	6.11
Ca^{2+}-Mt	—	7.36	1.54	28.9	—	0.119	—	16.48
Ca^{2+}-Mt –1.0	1.0	6.44	1.47	141.0	90.0(51.0)	0.183	0.023(12.6%)	5.20
Ca^{2+}-Mt –2.0	2.0	5.59	1.47	174.7	84.9(89.8)	0.189	0.039(20.6%)	4.34

[a] S_{ext} = external surface area, evaluated from the *t*-plot; the surface area of micropores (S_{micro}) is obtained by subtracting S_{ext} from the total surface area (S_{BET}).

[b] V_P = total porous volume.

[c] $V_{\mu P}$ = microporous volume, calculated by BJH method.

[d] APD = average pore diameter.

[e] After calcination at 773 **K** for 3h.

Figure Captions

Figure 1. FTIR of the Fe-pillared montmorillonite samples with different OH/Fe molar ratios.

Figure 2. Powder X-ray diffraction patterns of the initial montmorillonites and Fe-pillared samples.

Figure 3. Nitrogen adsorption isotherms of initial Na^{+}-Mt and pillared samples.

Figure 4. Schematic representation of the iron-delaminated pillared clays.

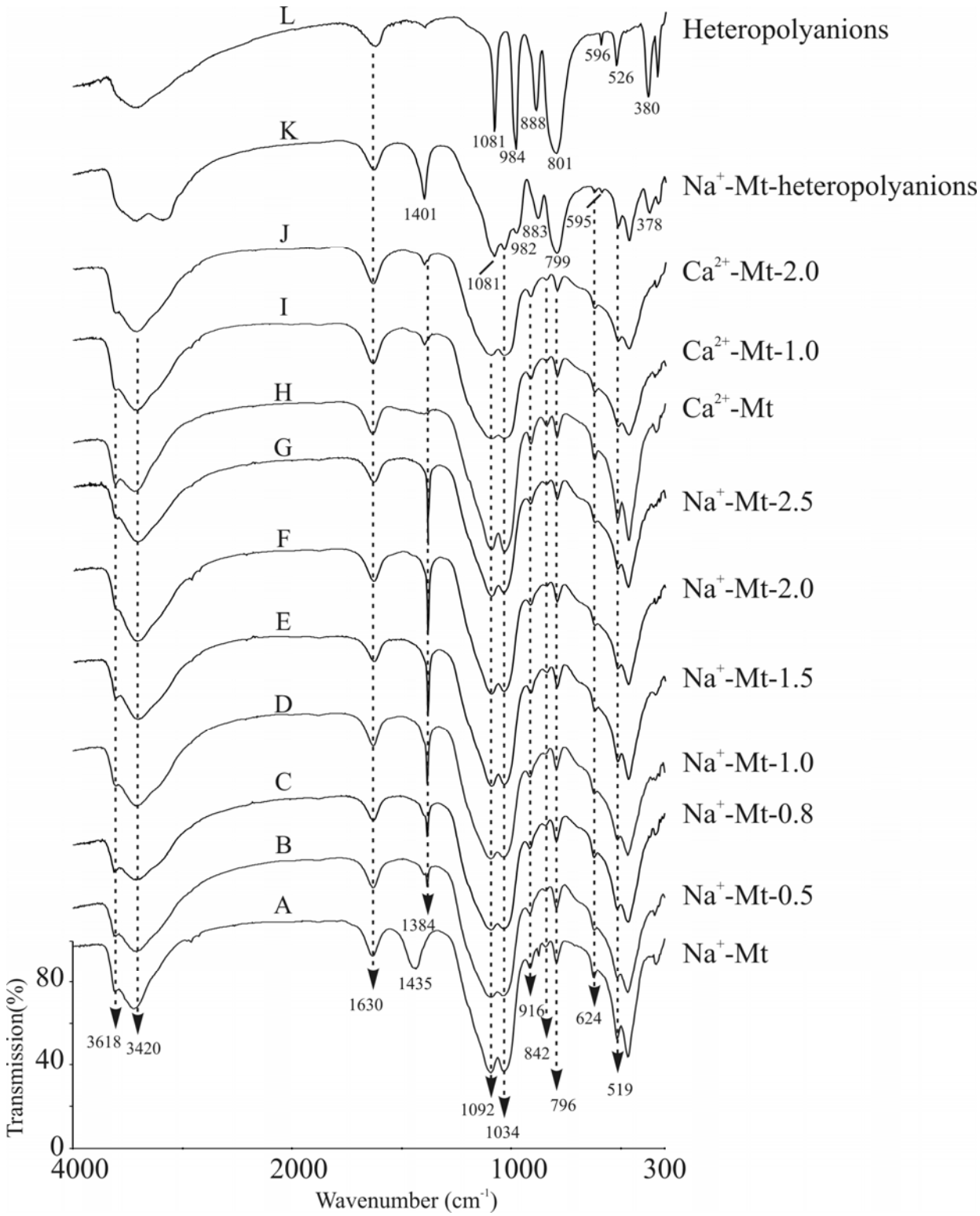

Fig. 1. FTIR of the Fe-pillared montmorillonite samples with different OH/Fe molar ratios.

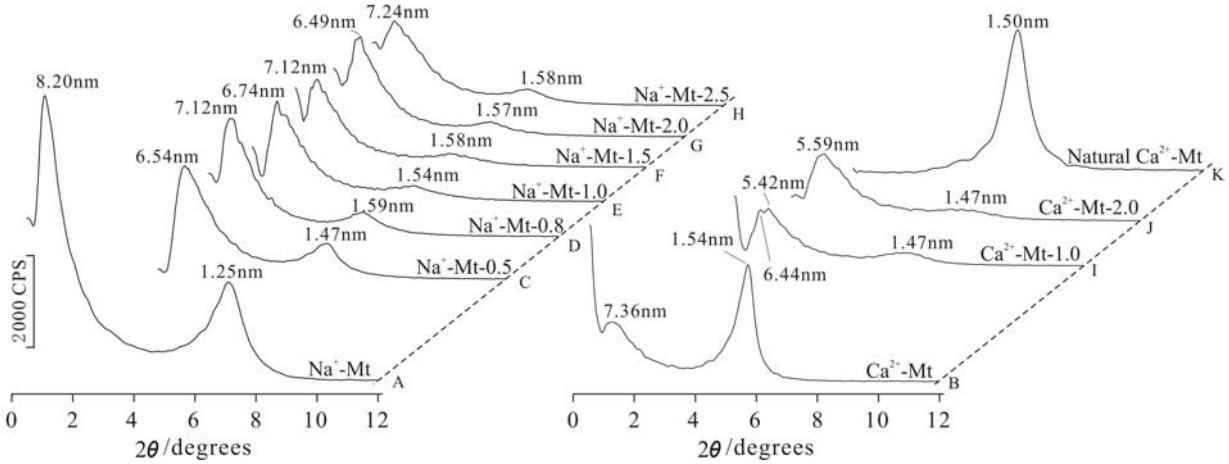

Fig. 2. Powder X-ray diffraction patterns for initial montmorillonites and Fe-pillared samples.

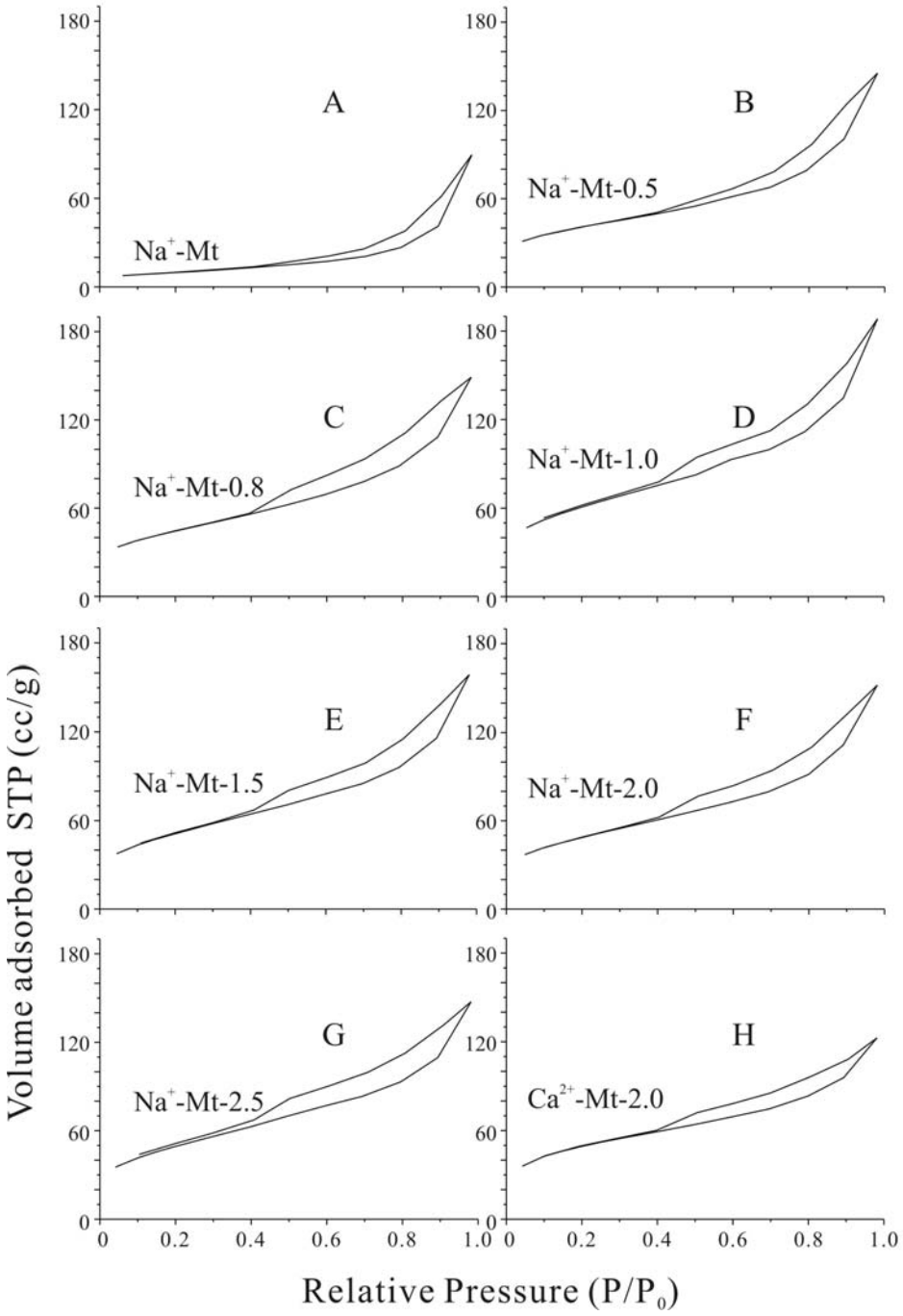

Fig. 3. Nitrogen adsorption isotherms of starting Na^{+}-Mt and pillared samples.

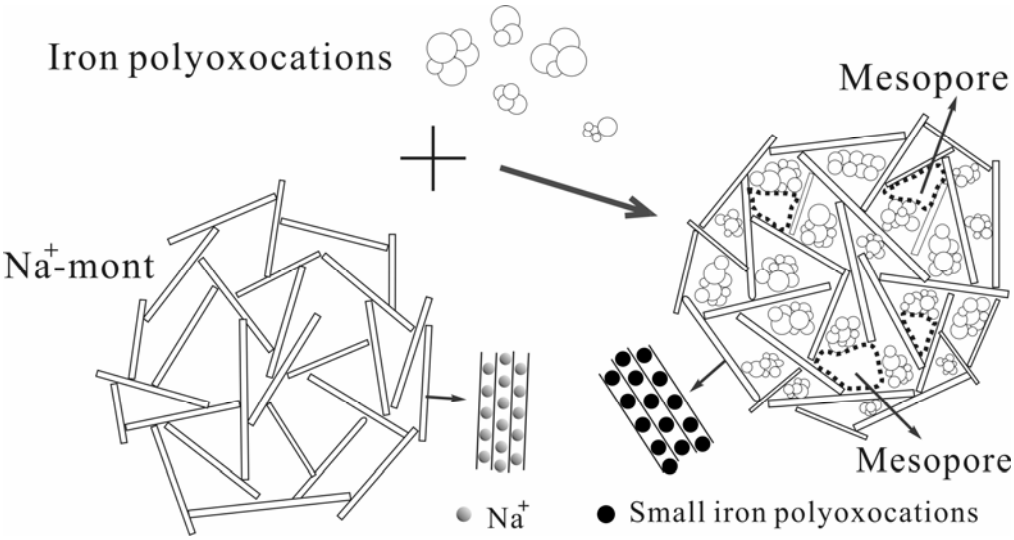

Fig. 4. Schematic representation of the iron delaminated pillared clays.